Fracture Mechanics of Concrete Structures
Proceedings FRAMCOS-3
AEDIFICATIO Publishers, D-79104 Freiburg, Germany

Fracture Process Zone of Composite Materials as Concrete

W. Yao, K. R. Wu
The State Key Laboratory of Concrete Materials Research,
Tongji University, Shanghai, P. R. China
Z. J. Li
Department of Civil and Structural Engineering, Hongkong University of Science & Technology, Hongkong, P. R. China

Abstract
In this paper, the mechanisms of formation and propagation of fracture process zone (FPZ) of concrete are elaborated. According to the tension softening character, a banding microcrack model (BMM) has been developed to describe the innate characteristic and pattern of FPZ. By using BMM, the size of FPZ can be quantitatively calculated. The calculated results are compared with the experimental measurements of other researchers.
Key words: Mechanisms of fracture, concrete, fracture process zone

1 Introduction

Since concrete is a heterogeneous material consisting of different phases, it is presented a nonlinear behavior characteristic in the region of inelastic zone around a propagating crack tip. Fracture process zone (FPZ) is such a result that led by the nonlinear phenomena. For the smaller concrete specimen, the size of FPZ is relatively larger, which even cover whole ligament. The failure of specimen will occur in the case that failure stress approach the ultimate strength of material. In this

case, the principles of LEFM are deterred to use for concrete and the related fracture criterion is invalid. In order to deal with this problem, mechanisms that responsible for FPZ in concrete have been studied. But the existing partial models give unsatisfactory results in evaluating the size of FPZ, due to these models following convention of the calculated model for the plastic zone of metallic materials, and not considering the innate characteristic of concrete. Therefore, to apply fracture mechanics to concrete, it is necessary to deeply understand and determine the FPZ, especially its size and establish a proper model.

2 Formation and propagation of FPZ

Series of tests to study the formation and propagation of FPZ have been carried out by acoustic emission (AE) technique. By using an 8 transducers to monitor AE events, and determining the time differences between the detection of each event at different transducer positions, the location of the AE event can be determined. It is found that in the initial stages of loading (Fig. 1a), AE signals originated at the region around of the crack tip. Due to the stress concentration, the stress in this region approaches tensile strength and causes microcracks. In Fig. 1b we can find that microcracks have random orientation with respect to the main crack plane, i.e. the possibility of microcracking is equal for surface and interior of the specimen. Mihashi (1991) obtained the similar results by using 3-D acoustic emission technique.

With the increasing of applied load, the amounts of microcracks also increase, and occur overlapping among the microcracks. A narrow band of internal cracks was detected within the measurement range by AE system (Fig. 1c, d). The damage zone, also termed as fracture process zone, which consists of microcracks, is formed. The length and width of band of internal microcracks continuously increased.

Near the peak load, With the continued accumulating of microcracks, it causes subcritical propagation of main crack, which also known as slow crack growth. Therefore, the presence of the FPZ results in stable crack growth before the peak load.

However, at the stage of peak load and thereafter, the microcracks in the FPZ have developed sufficiently, which make the shape and size of FPZ relative stable (Fig.1e, f). FPZ extends further rapidly, and leads to new crack surfaces. Effective intersection continuously decreases, but some AE events occurred ahead of the crack tip indicating ligament

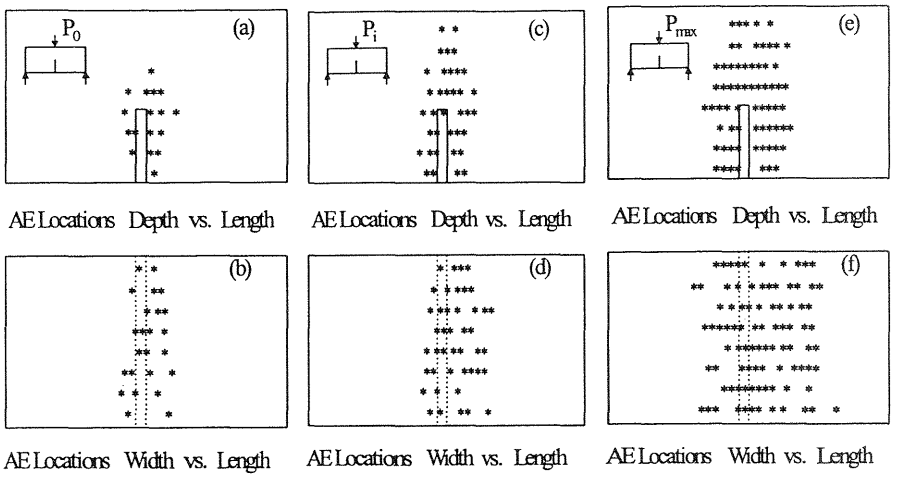

Fig. 1. Locations of internal microcracks for different loading stages detected by acoustic emission.

connections. Since some parts of crack surfaces may still be in contact after cracking, catastrophic failure of concrete structures immediately after the peak load is prevented. As a result, stress gradually decrease after the peak load, and a softening type of concrete stress-strain relationship is obtained. During the propagation of FPZ, in additional to microcracking, there are other mechanisms such as crack deflection, aggregate bridging, crack- face friction, crack tip blunting by voids, and crack branching, etc.

3 Banding Microcrack Model (BMM) of FPZ

Based upon the above mentioned AE phenomena, and considering the innate characteristic of concrete, a banding microcrack model (BMM) of FPZ is proposed. With the BMM, the size of FPZ can be quantitatively calculated.

3.1 Basic assumptions of BMM

1. An infinite concrete plate with Mode I crack under remote uniaxial tensile stress is considered (Fig. 2).
2. At the lower stress level σ_0, in the high stress region at the crack tip (between point O and A in the Fig. 2a), it will create well-distributed banding microcracks.

3. As applied load increasing (from σ_0 to σ_i), new microcracks continuously create, and the size of microcracks band increases (Fig. 2b). Depending on the transmit stress, FPZ is divided by two part, one is called as microcracks creation zone (from point O' to A'), another one is called as microcracks extension zone (from point O to O'). In the microcracks creation zone, the transmit stress is equal to tensile strength f_t ; while in the microcracks extension zone, due to tension softening, the transmit stress reduces as strain increasing. At this point, the tip of effective crack is moved to point O', while it behaves elastically in the materials outside the band of microcracks.
4. The tension softening responsible in the microcracks extension zone is determined by the uniaxial tensile test.
5. When the applied stress reaches the failure stress σ_N , the tip of effective crack moved to point O" , and microcracks band has fully extended (Fig. 2c). The transmit stress at point O decreases to zero, and point O becomes the actual start point of macro crack, while the transmit stress is still equal to tensile strength at the end point A".

According to above assumptions, in the state of Fig. 2c, the crack length is extended to $a+\Delta a$ from initial length a, where Δa is the length of microcrack extension zone at the critical state $K_I = K_{IC}$, and the transmit stress in the zone is σ (x). The stress state near the macrocrack tip is regarded as linear elastic fracture state with effective crack length being $a+\Delta a$ under sum of remote stress σ_N and cohesive pressure σ (x) between the microcracks, as shown in Fig. 3.

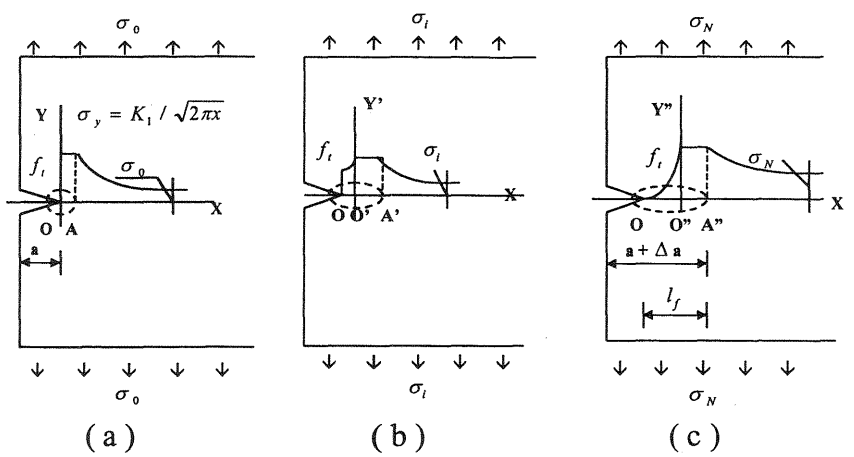

Fig. 2. Schematic illustration of BMM

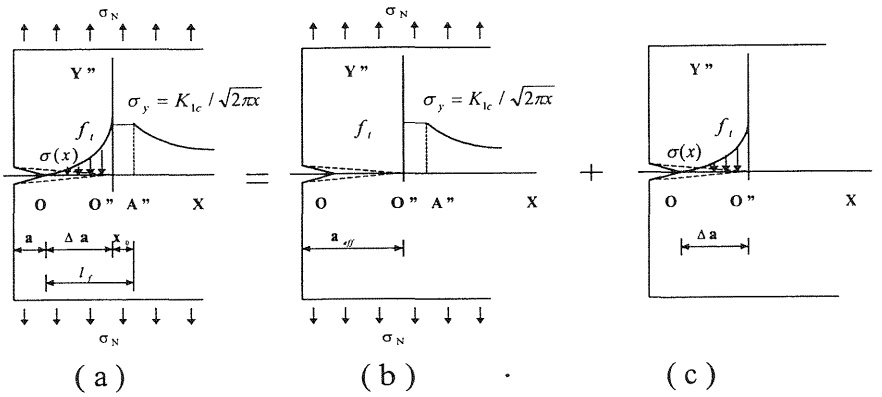

Fig. 3. Stress state (a) is sum of state (b) and state (c)

3.2 Length of FPZ (l_f)

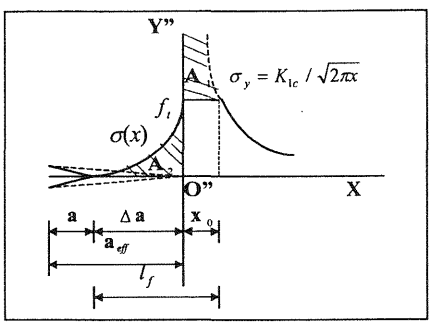

Fig. 4. Definition of l_f in critical state

Due to stress concentration, it will cause microcracking at the tip of Mode I crack, which led to stress redistribution in the microcracks zone. In concrete, the domain is presented as strain softening. According the superposition principle in Fig. 3 and the definition of FPZ, the length of FPZ can be calculated, as shown in Fig. 4.

In Fig. 4, $l_f = \Delta a + x_0$. The stress-strain relationship in Δa is determined by uniaxial tensile test. According to the study results of Yao (1995) and Wu (1997), the tension softening law is regarded as following:

$$\sigma = f_t \cdot e^{-kw} \qquad (1)$$

where k is softening degree, w is crack open displacement, f_t is tensile

strength. After function transformation, the cohesive pressure in the range of Δa is presented as follows

$$\sigma(x) = f_t \cdot e^{Cx} \tag{2}$$

where C is empirical coefficient, x is the length of crack zone, and is in mm. When $w = w_C$ (w_C is the crack separation corresponding to $\sigma(x) = 0$ and is termed the critical crack separation displacement), $x = -\Delta a$, so that $C = -k \cdot w_C / \Delta a$ is obtained. According to LEFM, we know

$$f_t = K_{1C} / \sqrt{2\pi x_0} \tag{3}$$

and

$$x_0 = \frac{1}{2\pi}\left(\frac{K_{1C}}{f_t}\right)^2 \tag{4}$$

Based upon the condition of load balance, area A_1 is equal to area A_2 (Fig. 4):

$$A_1 = \int_0^{x_0} \sigma_y dx - x_0 \cdot f_t = x_0 \cdot f_t \tag{5}$$

$$A_2 = \int_{\Delta a}^{0} f_t \cdot e^{cx} dx = \frac{f_t}{C}\left(1 - e^{-c\Delta a}\right) \tag{6}$$

By combining Eqs. (5) and (6) one obtain

$$\Delta a = -\ln(1 - Cx_0) / C \tag{7}$$

The value of Δa is then obtained by substituting $C = -k \cdot w_C / \Delta a$ into Eq. (7) as

$$\Delta a = k w_C x_0 / (1 - e^{-k w_C}) \tag{8}$$

The length of FPZ, namely l_f, can then be determined as

$$l_f = x_0 + \Delta a = x_0(1 + k w_C / (1 - e^{-k w_C})) \tag{9}$$

For metallic materials, due to yielding, $k \to 0$. It can be verified that the value of l_f is equal to $2x_0$, which is fit the length of modified yielding zone exactly. For concrete materials, Eq. (9) can be approximately expressed as follows by substituting the boundary condition $e^{-k w_C} \to 0$

$$l_f = x_0 + \Delta a = \frac{1 + k \cdot w_c}{2\pi}\left(\frac{K_{1c}}{f_t}\right)^2 \tag{10}$$

3.3 The width of FPZ (w_f)

To obtain the value of w_f, it is necessary to firstly determine the distribution of σ_y in perpendicular plane to the orientation of crack propagation. From Fig. 5, the value of σ_y at the crack tip is as

$$\sigma_y = \frac{K_1}{\sqrt{2\pi r}}\cos\frac{\theta}{2}\left[1 + \sin\frac{\theta}{2}\sin\frac{3\theta}{2}\right] \tag{11}$$

where r,θ is polar coordination.

Before microcracking, the distribution of σ_y in the plane of $\theta = 90^\circ$ near the crack tip is as follows:

$$\sigma_y\Big|_{\theta=90^\circ} = \frac{3K_1}{4\sqrt{\pi r}} \tag{12}$$

Supposing in the range of $r \le y_1$, the value of σ_y is equal to the tensile strength, then one can obtain

$$y_1 = \frac{9}{16\pi}\left(\frac{K_1}{f_t}\right)^2 \tag{13}$$

When $K_1 = K_{1c}$, y_1 has maximum value, and the width of FPZ can then be determined

$$W_f = 2y_1\Big|_{K_1=K_{1c}} = \frac{9}{8\pi}\left(\frac{K_{1c}}{f_t}\right)^2 \tag{14}$$

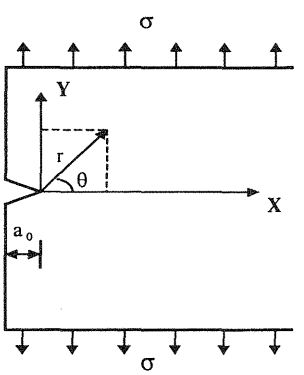

Fig. 5. Coordinate system in front of crack tip

4 Discussion and Conclusion

In the past, the size of FPZ was regarded as related to the specimen depth. For example, Alexander (1986, 1988) has reported that the length of FPZ is about 0.368~0.684 of specimen ligament. While the width of FPZ was regarded as proportion to the maximum aggregate size. Bazant (1983) reported that the width of FPZ is about three times of the maximum aggregate size, while Chhuy (1986) thought it is as wide as the maximum aggregate size and verified this using ultrasonic detective test. But the above views are thought to be lopsided. The reason is that the specimens tested is not large enough for the fully development of subcritical crack, which led to incorrect experimental results for the size of FPZ. In other words, the above reported results are not the terminal value of FPZ. Only when the specimen size is large enough, can the exact value of FPZ be determined by testing. Shah (1984) has studied the influence of specimen depth on the measured value of FPZ. He reported that with the increase of specimen ligament, the length of FPZ increases and gradually approaches to a constant value.

In Eqs. (10) and (14), as the coefficients k, w_C, and f_t are determined by directly tensile test, being material parameters, and K_{IC} being a true fracture parameter independent of size, the size of FPZ calculated by Eqs. (10) and (14) are also material parameters which are size independent. The following comparison is carried out with the data determined by some researchers .

Tian (1986) has tested a series of specimens with different depths but the same material, in which the maximum depth is about 2000 mm, and obtained a stable critical stress intensity factor using LEFM. The data are listed as: $a_0/h = 0.5$, $d_{max} = 20$ mm, $K_{IC} = 1.241$ MPa$\sqrt{m}$, $f_t = 2.46$ MPa. From regression analysis of the uniaxial test results of Yao (1995) and Gopalaratnam (1985), we suggest that the value of $k \cdot w_C$ equal 3. By substituting it into Eqs. (10) and (14), the length and width of FPZ can be obtained

$$l_f = \frac{1 + k \cdot w_c}{2\pi}\left(\frac{K_{Ic}}{f_t}\right)^2 = \frac{1+3}{2\pi}\left(\frac{1.241}{2.46}\right)^2 = 0.162 \text{ m} = 162 \text{ mm} \qquad (15)$$

and

$$w_f = \frac{9}{8\pi}\left(\frac{K_{IC}}{f_t}\right)^2 = 0.091 \text{ m} = 91 \text{ mm} \qquad (16)$$

In Table 1, some research results on FPZ by using different techniques and different geometry specimens are listed.

Table 1. Experimental measurements on the FPZ in concrete

No.	l_f (mm)	w_f (mm)	Testing method	Ref.
1	>114	-	Compliance measurements	Kabayashi (1985)
2	100	-	Three dimensional strain gauges	Chhuy (1986)
3	105	-	Acoustic emission	Izumi (1986)
4	160	120	Acoustic emission	Berthelot (1987)
5	>100	>100	Acoustic emission	Rossi (1989)
6	>100	-	Interferometry technique	Du (1989)

From Table 1, the results are similar, regardless of the geometry of specimen and the applied techniques. It indicates that the fracture process zone may have a substantial size.

Comparing with the calculated results of Eqs. (15), (16) and the measured ones of Table 1, it is found the data show similar to each other, which verify that the proposed model of FPZ in this paper is valid.

Moreover, the two results are showed size independent, indicating that the size of stable FPZ is a fundamental material property.

5 References

Alexander, M. G. and Blight, G. E. (1986) The use of small and large beams for evaluating concrete fracture characteristics, in **Fracture Toughness and Fracture Energy of Concrete** (ed. F.H. Wittmann), Elsevier Science Publishers B. V. , Amsterdam, 323-332.

Alexander, M. G. (1988) Use of ultrasonic pulse velocity for fracture testing of cemented materials. **Journal of Cement, Concrete and Aggregates, ASTM**, 1, 9-14.

Bazant, Z. P. and Oh, B. H. (1983) Crack band theory for fracture of concrete. **Materials and Structures, RILEM**, 16, 155-177.

Berthelot, J. -M. and Robert, J. -L. (1987) Modelling concrete damage by acoustic emission. **Journal of Acoustic Emission**, 1, 43-60.

Chhuy, S. , Cannard, G. and Acker, P. (1986) Experimental investigations into the damage of cement concrete with natural aggregate, in **Brittle Matrix Composites 1** (eds. A. M. Brandt and I. H. Marshall), Elsevier Applied Science, London, 341-354.

Du, J. , Hawkins, N. M. and Kobayashi, A. S. (1989) A hybrid analysis of fracture process zone in concrete, in **Fracture of Concrete and Rock: Recent Developments** (eds. S. P. Shah, S.E. Swartz, B. Barr), Elsevier Applied Science, London, 297-306.

Gopalaratnam, V. S. and Shah, S. P. (1985) Softening response of plain concrete in direct tension. **ACI Journal**, 3, 310-323.

Izumi, M. , Mihashi, H. and Nomura, N. (1986) Acoustic emission technique to evaluate fracture mechanics parameters of concrete, in **Fracture Toughness and Fracture Energy of Concrete** (ed. F. H. Wittmann), Elsevier Science Publishers B. V., Amsterdam, 259-268.

Kobayashi, A. S. , Hawkins, N. M. and Liaw, B. M. (1985) Fracture process zone of concrete, in **Applications of Fracture Mechanics to Cementitious Composites** (ed. S. P. Shah), Martinus Nijhoff Publishers, Dordrecht, 25-50.

Mihashi, H., Nomura, N. and Niiseki, S (1991) Influence of size on fracture process zone of concrete detected with dimensional acoustic emission technique. **Cement and Concrete Research,** 21, 737-744.

Rossi, P. , Robert, J. L. and Bruhat, D. (1989) Acoustic emission applied to study crack propagation in concrete. **Materiaux et Constructions,** 131, 374-383.

Shah, S. P. (1984) Dependence of concrete fracture toughness on specimen geometry and on composition, in **Fracture Mechanics of Concrete** (eds. A. Carpinteri and A. R. Ingraffea), Martinus Nijhoff Publisher, The Hugue, 113-135.

Tian, M. L. and Huang, S. M. (1986) Fracture toughness of concrete, in **Fracture Toughness and Fracture Energy** (ed. F. H. Wittmann), Elsevier Science Publishers B. V. , Amsterdam, 299-306.

Wu, K. R. and Yao, W. (1997) Analysis of damage mechanics and study of strain softening model for concrete in uniaxial stress state. **Journal of Dalian University of Technology,** Suppl. 1, 82-87.

Yao, W. and Wu, K. R. (1995) Study of tension softening of concrete. **Journal of Tongji University,** 23, 84-89.